

Chemical fronts in Hele-Shaw cells: Linear stability analysis based on the three-dimensional Stokes equations

Rainer Demuth and Eckart Meiburg^{a)}

Department of Mechanical and Environmental Engineering, University of California at Santa Barbara, Santa Barbara, California 93106

(Received 12 June 2002; accepted 19 November 2002; published 17 January 2003)

We present linear stability results based on the three-dimensional Stokes equations for chemically reacting, propagating fronts giving rise to an unstable density stratification in a Hele-Shaw cell. The results are compared with the experiments in M. Böckmann and S. C. Müller [Phys. Rev. Lett. **85**, 2506 (2000)], as well as with a corresponding linear stability analysis based on the Darcy equations that was performed in A. De Wit [Phys. Rev. Lett. **87**, 054502 (2001)]. The reason for the good agreement between these earlier Darcy data and the experimentally observed growth rates is found in the relatively low experimental value of the Rayleigh number, $Ra=79$, for which the flow is approximately of Poiseuille type. Already for Ra values as low as 300, we observe a discrepancy between the stability results based on the Darcy and Stokes equations, respectively, with the Darcy results overpredicting both the most amplified wavenumber, as well as the corresponding growth rate, by about a factor of two. This indicates that three-dimensional effects quickly gain importance as Ra increases, so that the stability analysis needs to be based on the full, three-dimensional Stokes equations. The stability results based on the Stokes equations furthermore demonstrate the stabilizing influences of both an increasing interfacial thickness, as well as increasing frontal propagation velocities, confirming the earlier Darcy-based findings by De Wit. An argument in terms of vorticity is forwarded to explain the latter effect. A more rapidly advancing front deposits vorticity over a wider layer of fluid particles, so that the concentrated regions of vorticity needed for rapid instability growth cannot form. Somewhat surprisingly, however, slowly propagating fronts are seen to be more unstable than nonreacting fronts of equivalent thickness, as the chemical reaction leads to the formation of more compact perturbations in the interfacial region. © 2003 American Institute of Physics. [DOI: 10.1063/1.1536972]

I. INTRODUCTION

Chemically reacting, propagating fronts in Hele-Shaw cells play a prominent role in the conversion of monomers into polymers (e.g., Pojman *et al.*,¹ Volpert *et al.*,² and McCaughey *et al.*³). In addition, they have gained importance in recent years as simple models for studying certain aspects of combustion phenomena (e.g., Professor P. Ronney's webpage http://cpl.usc.edu/liquid_flames/). De Wit⁴ provides an overview over several investigations that have addressed the linear stability of such fronts. As she points out, their stability depends crucially on the width and the speed of the propagating front. Employing a cubic reaction term, she applies the framework of Darcy's equations in order to compare both instability growth rates, as well as the dominant wavelengths, with experimental investigations of iodate-arsenous acid reaction fronts conducted by Böckmann and Müller⁵ in the Hele-Shaw configuration. For earlier investigations regarding the stability of such propagating fronts in planar gaps and axisymmetric tubes, cf. Refs. 6–8. For the parameter ranges in which the experiments by Böckmann and Müller⁵ were conducted, the stability analysis by De

Wit⁴ yields reasonably good quantitative agreement. Along similar lines, Martin *et al.*⁹ observe reasonably close agreement between a linear stability analysis based on the two-dimensional Navier–Stokes–Darcy equations and a three-dimensional lattice BGK simulation on one hand, and the experimental data of Ref. 5 on the other.

This observation of good quantitative agreement between the theoretical stability analysis based on Darcy's law by De Wit⁴ and the Hele-Shaw experiments by Böckmann and Müller⁵ is particularly interesting in light of related experimental and stability theoretical work by Fernandez *et al.*¹⁰ and Graf *et al.*,¹¹ respectively (cf. also the related work by Fernandez *et al.*¹²), for density driven instabilities at the interfaces of nonreacting, miscible fluids in Hele-Shaw cells. For this situation, a stability analysis based on the gap-averaged Hele-Shaw equations, i.e., Darcy's law yields approximate quantitative agreement with the Hele-Shaw experiments only for fairly small values of the governing dimensionless parameter in the form of a Rayleigh number Ra . For Ra values above $O(100)$, the growth rates and dominant wavenumbers obtained from Darcy's law, significantly overpredict the experimentally observed values. The reason for this discrepancy is found to lie in the fact that at large Ra values the velocity profiles associated with the interfacial instability are not of the Poiseuille type. As a result, the

^{a)} Author to whom correspondence should be addressed. Electronic mail: meiburg@engineering.ucsb.edu

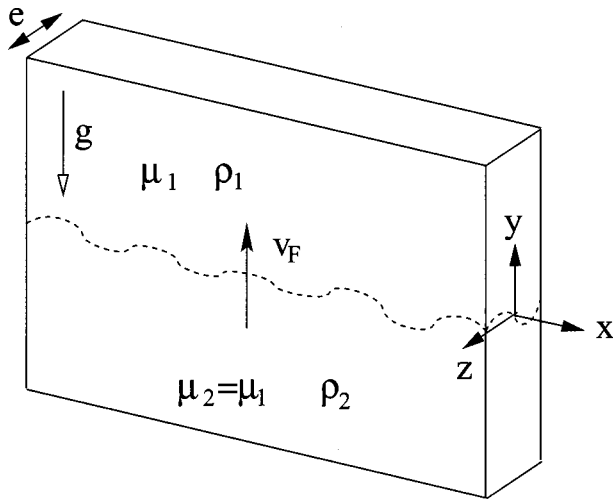


FIG. 1. Sketch of the upward propagating, unstable density front between two chemically reacting fluids.

gap-averaging procedure by which Darcy's law is derived for Hele-Shaw flows is not applicable at high Ra values, so that the stability analysis has to be based on the full three-dimensional Stokes equations instead. As the results by Graf *et al.* show, such an analysis yields excellent agreement with the Hele-Shaw experiments by Fernandez *et al.* across the entire range of Ra .

With the above observations for nonreacting unstable density interfaces in mind, the question arises regarding the range of parameters for which the Darcy approach is applicable with respect to the stability of reacting fronts. In order to address this issue, the linear stability analysis by Graf *et al.* of the three-dimensional Stokes equations will be extended below to the case of reacting fronts. Its results will subsequently be compared with those of the Darcy approach, in order to establish the range of applicability. After establishing the governing equations along with the corresponding dimensionless parameters, we will separately investigate the influence of the Rayleigh number, the front thickness, and the front propagation velocity.

II. PHYSICAL PROBLEM AND GOVERNING EQUATIONS

The goal is to investigate the linear stability of an upward propagating, unstable density front that separates two chemically reacting fluids in a vertically oriented Hele-Shaw cell of gap width e , as sketched in Fig. 1. This situation corresponds to the experimental setup studied by Böckmann and Müller,⁵ and analyzed by De Wit⁴ on the basis of Darcy's equation.

A. Three-dimensional Stokes equations

We base the linear stability investigation on the three-dimensional Stokes equations for incompressible flow. In following De Wit,⁴ we assume the Boussinesq approximation, so that density variations enter only into the buoyancy term.

The two fluids are assumed to be miscible in all proportions. Under these conditions, we obtain for the conservation of mass, momentum and species

$$\nabla \cdot \mathbf{u} = 0, \quad (1)$$

$$\nabla p = \mu \nabla^2 \mathbf{u} + \rho \mathbf{g}, \quad (2)$$

$$\frac{\partial c}{\partial t} + \mathbf{u} \cdot \nabla c = D \nabla^2 c + f(c). \quad (3)$$

The dependent flow variables consist of the velocity \mathbf{u} , the pressure p , and the concentration c of the heavier fluid 1. The density ρ is taken to be a linear function of the concentration

$$\rho = \rho_2 + (\rho_1 - \rho_2)c/c_1, \quad (4)$$

whereas the viscosity μ and the diffusion coefficient D are considered constant. For the reaction term in the concentration equation we employ the same, cubic form as in the investigation by De Wit⁴

$$f(c) = -\gamma c(c - c_1)(c + c_2). \quad (5)$$

In order to render the above set of governing equations dimensionless, we introduce a characteristic length L^* , velocity U^* , time T^* , pressure P^* , density difference R^* and concentration c^* as follows, cf. Graf *et al.*:¹¹

$$L^* = e, \quad (6)$$

$$T^* = \frac{\mu}{\Delta \rho \cdot g \cdot e}, \quad (7)$$

$$U^* = \frac{\Delta \rho \cdot g \cdot e^2}{\mu}, \quad (8)$$

$$P^* = \Delta \rho \cdot g \cdot e, \quad (9)$$

$$R^* = \Delta \rho, \quad (10)$$

$$c^* = c_1. \quad (11)$$

In a reference frame that moves upwards with the velocity v_F of the chemical reaction front, we thus obtain the following set of dimensionless governing equations:

$$\nabla \cdot \mathbf{u} = 0, \quad (12)$$

$$\nabla p = \nabla^2 \mathbf{u} + c \nabla y, \quad (13)$$

$$\frac{\partial c}{\partial t} + \mathbf{u} \cdot \nabla c + v_F \frac{\partial c}{\partial y} = \frac{1}{Ra} \nabla^2 c - \alpha c(c - 1)(c + d). \quad (14)$$

Here the Rayleigh number Ra

$$Ra = \frac{\Delta \rho g e^3}{D \mu}, \quad (15)$$

provides a relative measure of the destabilizing buoyancy forces and the stabilizing effects of diffusion and viscosity. Note that in the stability analysis of De Wit⁴ all lengths are referred to the purely diffusive scale D/U , so that a Rayleigh number does not appear.

As explained in detail by De Wit,⁴ the above form of the reaction term represents a chemical reaction with two steady states, cf. Refs. 13–16. It gives rise to the concentration ratio d

$$d = \frac{c_2}{c_1}, \tag{16}$$

and a dimensionless kinetic constant α

$$\alpha = \frac{c_1^2 \gamma \mu}{\Delta \rho g e}, \tag{17}$$

which indicates the ratio of the time scales on which buoyancy-induced motion and chemical reaction take place, respectively. Note that, due to the fact that we choose the gap width as the characteristic length scale, our dimensionless kinetic constant is defined differently from the one of De Wit,⁴ who employs a diffusive length scale instead. The propagation velocity v_F of the front, and its thickness Δy between the concentration values c_a and c_b are related to α and Ra as

$$v_F = \sqrt{\frac{\alpha}{2 \cdot Ra}} (1 + 2d), \tag{18}$$

$$\Delta y = \frac{1}{\sqrt{\frac{\alpha \cdot Ra}{2}}} \ln \left(\frac{c_a(1 - c_b)}{c_b(1 - c_a)} \right). \tag{19}$$

B. Linear stability problem

For fluid at rest everywhere, the system of dimensionless governing equations (12)–(14) gives rise to a steady base state concentration profile

$$c(y) = \frac{1}{1 + \exp \left(\sqrt{\frac{\alpha \cdot Ra}{2}} y \right)}. \tag{20}$$

We consider small perturbations to this base state of the form

$$\begin{pmatrix} u' \\ v' \\ w' \\ p' \\ c' \end{pmatrix} (x, y, z, t) = \begin{pmatrix} \hat{u}(y, z) \sin(\beta x) \\ \hat{v}(y, z) \cos(\beta x) \\ \hat{w}(y, z) \cos(\beta x) \\ \hat{p}(y, z) \cos(\beta x) \\ \hat{c}(y, z) \cos(\beta x) \end{pmatrix} e^{\sigma t}. \tag{21}$$

By substituting the base state and the perturbations into the system of governing equations, subtracting out the base state, and linearizing, we obtain the following generalized eigenvalue problem:

$$\underline{A} \phi = \sigma \underline{B} \phi, \tag{22}$$

for the growth rate σ and the eigenvector ϕ

$$\phi = \begin{pmatrix} \hat{u} \\ \hat{v} \\ \hat{w} \\ \hat{p} \\ \hat{c} \end{pmatrix}. \tag{23}$$

This system is solved numerically in order to compute the eigenvalues σ along with the eigenfunctions \hat{u} , \hat{v} , \hat{w} , \hat{p} , and

\hat{c} as functions of the spanwise wave number β , for various combinations of Ra , α , and d . Towards this end, we employ an iterative Arnoldi-method, as implemented in the public domain software package ARPACK. Regarding numerical discretization, validation, and convergence acceleration, we follow the same steps as Graf *et al.*¹¹ It needs to be mentioned that converged results for both the eigenvalue as well as the eigenvector could not be obtained for all parameter combinations, which somewhat limited our ability to explore certain parts of the parameter space.

C. Darcy's law

For comparison purposes, we also implement the corresponding stability problem based on a Darcy description. We nondimensionalize the governing equations in the same way as above. After casting them in the familiar streamfunction-vorticity formulation, we obtain

$$\nabla^2 \psi + \omega = 0, \tag{24}$$

$$12\omega + \frac{\partial c}{\partial x} = 0, \tag{25}$$

$$\frac{\partial c}{\partial t} + \mathbf{u} \cdot \nabla c + v_F \frac{\partial c}{\partial y} = \frac{1}{Ra} \nabla^2 c - \alpha c(c-1)(c+d). \tag{26}$$

For small perturbations of the form

$$\psi'(x, y, t) = \hat{\psi}(y) \cdot \sin(\beta x) \cdot e^{\sigma t}, \tag{27}$$

$$\omega'(x, y, t) = \hat{\omega}(y) \cdot \sin(\beta x) \cdot e^{\sigma t}, \tag{28}$$

$$c'(x, y, t) = \hat{c}(y) \cdot \cos(\beta x) \cdot e^{\sigma t}, \tag{29}$$

we again obtain a generalized eigenvalue system of the same form as in (22), with the eigenvector ϕ

$$\phi = \begin{pmatrix} \hat{\psi} \\ \hat{\omega} \\ \hat{c} \end{pmatrix}. \tag{30}$$

This system can be solved numerically in complete analogy to the corresponding Stokes problem.

III. RESULTS

As validation of our linear stability solution procedures, we provide a comparison of a representative dispersion relation with corresponding experimental data of Böckmann and Müller.⁵ These same experimental data also served for comparison with the stability results of De Wit.⁴ The experimental parameters for this case are $\Delta \rho / \rho_1 = 1.3 \times 10^{-4}$, $e = 0.05$ cm, $D = 2.04 \times 10^{-5}$ cm²/s, $\nu = 0.0099$ cm²/s, $g = 980.665$ cm/s², $[\text{IO}_3^-]_0 = 4.8 \times 10^{-3}$ M, $k_a = 4.5 \times 10^3$ M⁻³/s, $k_b = 4.510 \times 10^8$ M⁻⁴/s, and $[\text{H}^+] = 6.45 \times 10^{-3}$ M. With $c_1 = [\text{IO}_3^-]_0$, $c_2 = k_a / k_b$, and $\gamma = k_b [\text{H}^+]^2$, we arrive at the dimensionless parameter values $Ra = 79$, $v_F = 6.5 \cdot 10^{-2}$, and $\Delta y = 1.79$. Here we determine the thickness of the reaction front from $c_a = 0.01$ and $c_b = 0.99$. Both the Stokes as well as the Darcy results qualitatively reproduce the experimental data, cf. Fig. 2, with the Stokes results providing somewhat better quantitative agreement. Furthermore, the present

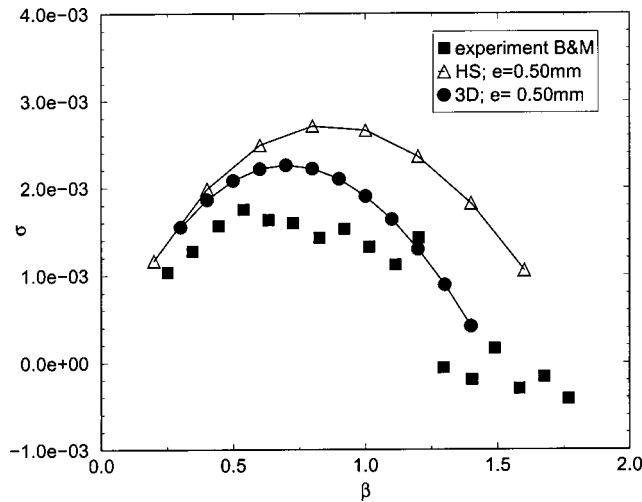


FIG. 2. Comparison of the dispersion relations obtained from the Stokes equations (circles) and Darcy's law (triangles), respectively, with the experimental data of Böckmann and Müller (Ref. 6) (squares). While the Stokes data are seen to agree somewhat better with the experiments, the Darcy data show reasonable agreement as well for the present, low value of $Ra = 79$, as was also observed by De Wit (Ref. 5).

Darcy results agree with the corresponding stability results reported by De Wit.⁴ The present stability results based on the Stokes and Darcy approaches exhibit the same tendencies as observed earlier by Graf *et al.*¹¹ for the nonreacting case, in that both the growth rates as well as the wavenumbers of maximum and neutral growth are somewhat overpredicted by the Darcy approach, even at the present, moderate Ra value of $O(100)$. However, this Ra value is sufficiently small for the discrepancy between the Stokes and the Darcy results to be minor, which explains the good agreement found by De Wit⁴ between her linear stability results based on the Darcy approach and the experimental data of Böckmann and Müller.⁵

As a next step, we raise Ra , in order to check if the increasingly poor agreement between Darcy and Stokes results observed by Graf *et al.* for nonreacting flows at higher Ra translates to the chemically reacting case as well. Figure 3 presents Darcy and Stokes dispersion relations data for three different values of Ra . Notice that the front thickness as well varies with Ra . The figure clearly demonstrates that even at Ra values as low as 300, the discrepancy between Darcy and Stokes results is already significant. The Darcy results overpredict not only the maximum growth rate by a factor of two, but also the most amplified and the cutoff wavenumbers. This suggests that, as for nonreacting flows, three-dimensional effects quickly increase with Ra , so that the Poiseuille flow assumption underlying the Darcy approach for Hele-Shaw flows becomes less and less applicable. For this reason, in the following we will present exclusively data based on the linearized Stokes equations.

In order to assess the role that the front thickness plays in the growth of the interfacial instability, we keep the front velocity and the Rayleigh number at the constant values of $v_p = 6.5 \cdot 10^{-2}$ and $Ra = 120$, respectively, while varying the thickness of the reaction front, cf. Fig. 4. The stability data show an increasing front thickness to be stabilizing. This

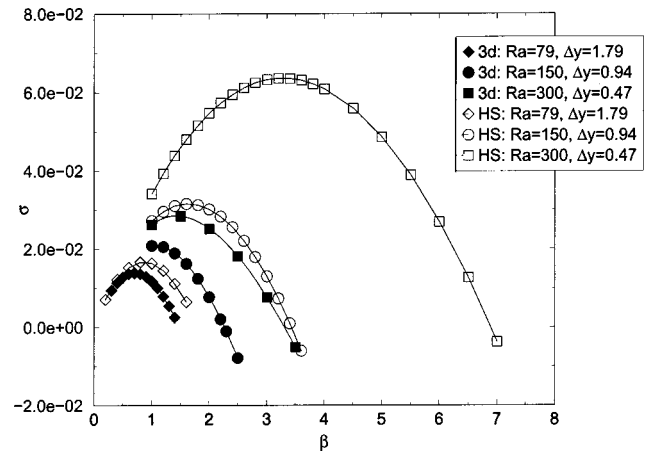


FIG. 3. Comparison of dispersion relations obtained from Darcy's law (open symbols) and the three-dimensional Stokes equations (solid symbols), for three different combinations of Ra and front thickness. Even for Ra values as low as 300, the Darcy results overpredict the maximum growth rate, as well as the most amplified and the cutoff wavenumbers, by roughly a factor of two.

observation is in agreement with the findings of Graf *et al.*¹¹ for the nonreacting case, for both Darcy and Stokes based analyses. A direct comparison with the Darcy analysis of De Wit is not possible, since she does not present results for which the frontal propagation velocity is held constant.

Figure 5 depicts Stokes based stability data for three different front propagation velocities, with Ra held constant at 120, and Δy_F fixed at 1.8. The lowest front velocity is seen to result in the highest growth rate. This observation that the front velocity is stabilizing is in agreement with the corresponding Darcy results obtained by De Wit.⁴ It can be understood in terms of the underlying vorticity dynamics, which drives the growth of the instability. Throughout the evolution of the flow, vorticity is generated and instantaneously "deposited" at those fluid elements that exhibit a

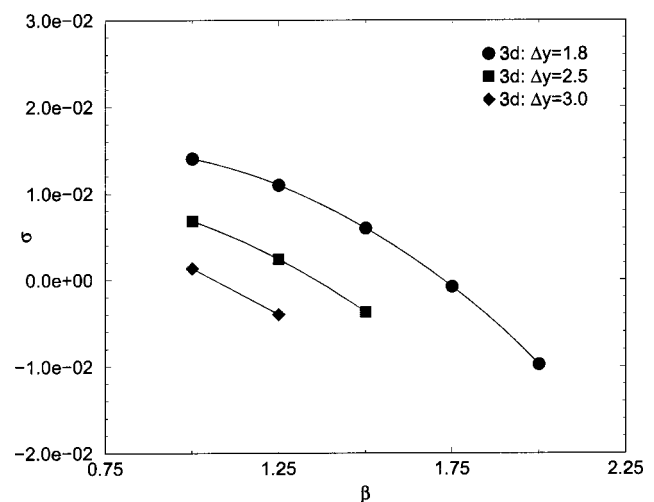


FIG. 4. Effect of variable front thickness on the instability growth rates, for constant Rayleigh number and front propagation speed. In agreement with the Darcy and Stokes results of Graf *et al.* (Ref. 12) for the nonreacting case, the present Stokes results show an increasing front thickness to be stabilizing.

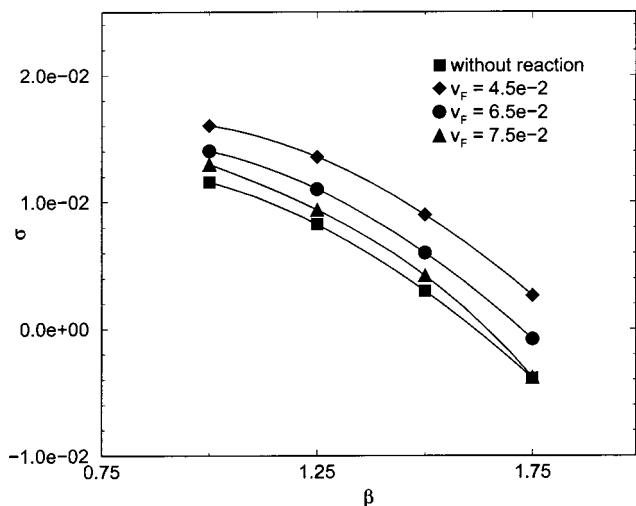


FIG. 5. Effect of the front velocity on the instability growth rates, for constant front thickness and Ra value. Larger front propagation velocities are seen to lead to lower growth rates. This is due to the less pronounced accumulation of vorticity near the interface, as explained in the text, which prevents the effective amplification of the instability. On the other hand, the nonreacting flow with identical front thickness displays the lowest growth rates.

horizontal density gradient, i.e., at those fluid elements located within the perturbed front. If the front propagates slowly, this vorticity has the opportunity to accumulate in a narrow region over time, so that regions of concentrated vorticity emerge that can effectively amplify the evolving instability. If, on the other hand, the front propagates more rapidly, fluid elements at which vorticity was deposited earlier will quickly be left behind by the front. Consequently, regions of concentrated vorticity do not form as effectively, which results in a less pronounced growth of the frontal instability. In other words, the faster the front propagates, the more spread out the overall vorticity field will become, so that the high vorticity concentrations needed for a rapid growth of the instability cannot be achieved.

On the basis of the above argument, one might assume that the case of the nonreacting front should then exhibit the fastest growth rate, because here the vorticity can accumulate in an “optimal” way. However, Fig. 5 demonstrates that the case of an identical front thickness, but without chemical reaction is characterized by growth rates that are lower than those of all three reacting cases. The explanation for this perhaps unexpected behavior can be found in the eigenfunctions for the nonreacting and reacting cases, displayed in Figs. 6 and 7, respectively. These show that, for identical front thicknesses, the chemical reaction counteracts the effects of diffusion, thereby giving rise to significantly more concentrated perturbations than the nonreacting case. As a result, for slowly propagating fronts the perturbation vorticity can become more concentrated than for the nonreacting case, thereby amplifying the instability more effectively.

IV. SUMMARY

For nonreacting, unstable miscible density interfaces in Hele-Shaw cells, Graf *et al.*¹¹ had found a growing discrep-

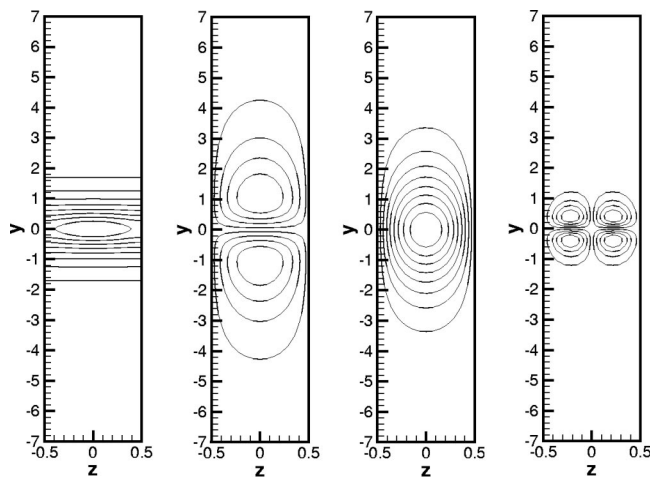


FIG. 6. Eigenfunctions of \hat{c} , \hat{u} , \hat{v} , and $\hat{\omega}$ for the nonreacting case. The effects of diffusion lead to a spreading of the eigenfunctions over a fairly large vertical distance.

ancy between linear stability results based on Darcy’s and Stokes equations, respectively, as the Rayleigh number increased. Specifically, for large values of Ra the Darcy results were seen to vastly overpredict both the most amplified wavenumbers, as well as the corresponding growth rates. This observation motivated us to revisit the experiments by Böckmann and Müller⁵ involving chemically reacting, propagating fronts in a Hele-Shaw cell, for which the linear stability analysis by De Wit,⁴ which is based on the Darcy equations, shows reasonable agreement. The reason for this good agreement is found in the relatively low value of $Ra = 79$ in the experiment, which leads to a predominantly Poiseuille-type flow behavior, so that the Darcy equation is largely applicable.

However, already for Ra values as low as 300, we observed a significant discrepancy between the stability results based on the Darcy and Stokes equations, respectively, with the Darcy results overpredicting both the most amplified

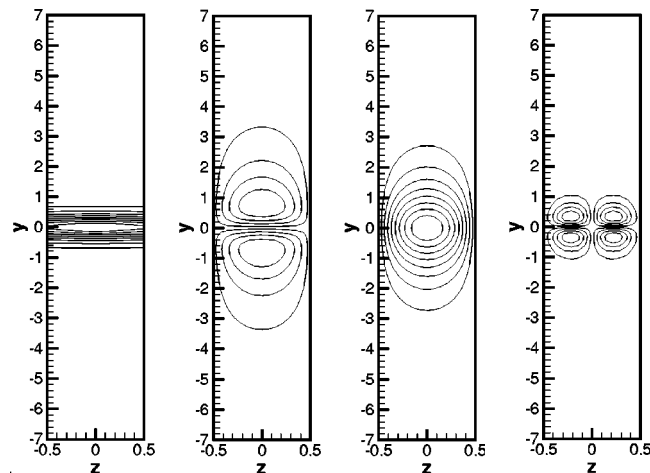


FIG. 7. Eigenfunctions of \hat{c} , \hat{u} , \hat{v} , and $\hat{\omega}$ for the chemically reacting case with $v_F = 4.5 \cdot 10^{-2}$. The chemical reaction leads to much more compact eigenfunctions, which result in a more effective amplification of the instability.

wavenumber, as well as the corresponding growth rate, by about a factor of 2. This indicates that three-dimensional effects quickly gain importance as Ra increases, so that the stability analysis needs to be based on the full, three-dimensional Stokes equations. The stability results based on the Stokes equations furthermore demonstrate the stabilizing influences of both an increasing interfacial thickness, as well as increasing frontal propagation velocities. A vorticity based argument is forwarded to explain the latter effect. Essentially, a more rapidly propagating front deposits vorticity over a wider layer of fluid particles, so that the concentrated regions of vorticity needed for rapid instability growth cannot form. Somewhat surprisingly, however, slowly propagating fronts are more unstable than nonreacting fronts of equivalent thickness, as the chemical reaction leads to the formation of more compact perturbations in the interfacial region.

ACKNOWLEDGMENT

The authors gratefully acknowledge discussions with A. De Wit, G. M. Homsy, and P. Ronney. This work is supported through the NASA Microgravity and the NSF-ITR Programs, as well as by an NSF equipment grant.

- ¹J. A. Pojman, V. M. Ilyashenko, and A. M. Khan, "Free-radical frontal polymerization: Self-propagating thermal reaction waves," *J. Chem. Soc., Faraday Trans.* **92**, 2825 (1996).
²V. A. Volpert, V. A. Volpert, J. A. Pojman, and S. E. Solov'yov, "Hydrodynamic stability of a polymerization front," *Eur. J. Appl. Math.* **7**, 303 (1996).
³B. McCaughey, C. Simmons, and V. A. Volpert, "The effect of convection

on a propagating front with a liquid product: Comparison of theory and experiments," *Chaos* **8**, 520 (1998).

- ⁴A. De Wit, "Fingering of chemical fronts in porous media," *Phys. Rev. Lett.* **87**, 054502 (2001).
⁵M. Böckmann and S. C. Müller, "Growth rates of the buoyancy-driven instability of an autocatalytic reaction front in a narrow cell," *Phys. Rev. Lett.* **85**, 2506 (2000).
⁶J. A. Pojman, I. R. Epstein, T. J. McManus, and K. Showalter, "Convective effects on chemical waves. 2. Simple convection in the iodate-arsenous acid system," *J. Phys. Chem.* **95**, 1299 (1991).
⁷J. Masere, D. A. Vasquez, B. F. Edwards, J. W. Wilder, and K. Showalter, "Nonaxisymmetric and axisymmetric convection in propagating reaction-diffusion fronts," *J. Phys. Chem.* **98**, 6595 (1994).
⁸M. R. Carey, S. W. Morris, and P. Kolodner, "Convective fingering of an autocatalytic reaction front," *Phys. Rev. E* **53**, 6012 (1996).
⁹J. Martin, N. Rakotomalala, D. Salin, and M. Böckmann, "Buoyancy-driven instability of an autocatalytic reaction front in a Hele-Shaw cell," *Phys. Rev. E* **65**, 051605 (2002).
¹⁰J. Fernandez, P. Kurowski, P. Petitjeans, and E. Meiburg, "Density-driven, unstable flows of miscible fluids in a Hele-Shaw cell," *J. Fluid Mech.* **451**, 239 (2002).
¹¹F. Graf, E. Meiburg, and C. Härtel, "Density-driven instabilities of miscible fluids in a Hele-Shaw cell: Linear stability of the three-dimensional Stokes equations," *J. Fluid Mech.* **451**, 261 (2002).
¹²J. Fernandez, P. Kurowski, L. Limat, and P. Petitjeans, "Wavelength selection of fingering instability inside Hele-Shaw cells," *Phys. Fluids* **13**, 3120 (2001).
¹³A. Nitzan, P. Ortoleva, and J. Ross, "Nucleation in systems with multiple stationary states," *Faraday Symp. Chem. Soc.* **9**, 241 (1974).
¹⁴G. A. Papsin, A. Hanna, and K. Showalter, "Bistability in the oxidation of arsenous acid," *J. Phys. Chem.* **85**, 2575 (1981).
¹⁵A. Hanna, A. Saul, and K. Showalter, "Detailed studies of propagating wave fronts in the iodate oxidation of arsenous acid," *J. Am. Chem. Soc.* **104**, 3838 (1982).
¹⁶A. Saul and K. Showalter, in *Oscillations and Traveling Waves in Chemical Systems*, edited by R. J. Field and M. Burger (Wiley, New York, 1985).